The chaotic dripping faucet

P. Coullet[*], L. Mahadevan[†] and C. Riera[*]

[*] *Institut Non Lineaire de Nice, UMR CNRS 129, 1361 Route des Lucioles, 06560 Valbonne, France*
[†] *Department of Mechanical Engineering, 1-310, M.I.T., 77 Mass. Ave., Cambridge, MA 02139, USA*

We propose a simple model for the chaotic dripping of a faucet in terms of a return map constructed by analyzing the stability of a pendant drop. The return map couples two classical normal forms, an Andronov saddle-node bifurcation, and a Shilnikov homoclinic bifurcation. The former corresponds to the initiation of the instability when the drop volume exceed a critical value set by the balance between surface tension and gravity, while the latter models the global reinjection associated with pinch-off that eventually return the drop to a state close to its original unstable configuration. The results obtained using the return map are consistent with those of numerical simulations of the governing PDEs and prior experiments, and show periodic and quasi-periodic dripping at low and high flow rates, and chaotic behavior at intermediate flow rates.

Drop formation is an everyday phenomena with a scientific history going back atleast to Mariotte [1] who noticed that a stream of water flowing from a faucet breaks into drops, and attributed it to gravity and external forces. Much later the studies of Young [2] and Laplace [3] lead to the realization that surface tension as the destabilizing agent. Ever since then, and through recent times the subject has been active, with current interests centered around singularity formation in free-surface flows [4]. Here we focus on the aspect of the problem that provided a stimulus to early studies on chaos [5], the transition to chaotic dripping in a faucet. Although the subject of many experimental and theoretical papers (see [6] for a recent example along with a review of earlier work), nearly all work in this area treats the system as a relaxation oscillator using a phenomenologically motivated equation, instead of treating the hydrodynamics in a rational way. A recent exception is the work of Fuchikami et al [7], who simulated the chaotic behavior using an asymptotically correct hydrodynamic model. Our aim is to provide a minimal model based on fluid mechanics to explain the dynamics of a dripping faucet.

In order to do so, we first consider the case when the flow rate is very small, so that a drop remains attached to the faucet until its volume exceeds a threshold V_c. For a narrow faucet of radius R, drops with a volume less than V_c are stable and axisymmetric [8,9]; for wider faucets, one can have non axisymetric stable drops [10], leading to more complex dripping patterns, but we will not consider this case here. The shape of an axisymmetric pendant drop is determined by the minimizing the sum of its gravitational and surface energy subject to the constraint of constant volume, and leads to the well-known Laplace-Young equation [9]. Equivalently, one may write down an equation for the balance of vertical forces, along with kinematic equations for the shape of the interface, leading to the following system of dimensionless ODEs

$$\begin{cases} \dfrac{d\theta}{ds} &= \dfrac{\cos\theta}{r} - z \\ \dfrac{dz}{ds} &= -\cos\theta \\ \dfrac{dr}{ds} &= \sin\theta \end{cases} \qquad (1)$$

Here the variables r, s, θ and z are defined in FIG. 1.a for a fluid drop with surface tension Γ, and density ρ in a gravitational field g. To make the equations dimensionless, we have scaled all lengths by the capillary length $l_0 = \sqrt{\Gamma/g\rho}$, all masses by $m_0 = \rho l_0^3$ and pressure by $P_0 = \sqrt{\rho\Gamma g}$. For later use, we scale all times by $t_o = (\Gamma/\rho g^3)^{1/4}$. For water at $20^0 C$, $l_0 = 0.27 cm, m_0 = 0.020 g, P_0 = 270 dyn/cm^2, t_0 = 0.017s$.

The boundary conditions at the bottom of the drop are $r(0) = 0$, $\theta(0) = \pi/2$ and $z(0) = P_b$ where P_b is the unknown hydrostatic pressure at the bottom of the drop. Choosing a value for P_b, we integrate (1) as an initial value problem till we satisfy the boundary condition $r = R$ (we choose $R = 1$; in dimensional terms $R = l_0$), and use a shooting method to determine P_b for a given drop volume $V = \int \pi r^2 dz$. Of the various shapes of static pendant drops that exist for a given volume, shown in FIG. 1.b, only the branch starting at the origin with a positive slope is stable, so that there is a critical drop volume V_c at which the weight of the drop just balances the force due to surface tension. The resulting instability when $V > V_c$ results from the "collision" of two stationary solutions, a stable one and an unstable one, and corresponds to a saddle-node bifurcation, as we shall see.

To understand the dynamics of this instability, we consider the hydrodynamical equations linearized about the stationary pendant drop. Since much of the behavior during dripping involves the dynamics of slender liquid jets, we use a lubrication model for the fluid, embodied in a Lagrangian approach. The inherent assumptions in this are the

following: (i) the drop remains axisymmetric during its motion, (ii) the radial component of the fluid velocity is negligible compared to the axial component which depends on z alone, (iii) there is no overturning of the interface which is assumed to be a graph in the axial variable z. These assumptions are asymptotically valid for slender drops of large viscosity, but recently simulations of the resulting low-order equations have shown good agreement with experiments even for low viscosity drops [11]. The above assumptions also imply that there is no exchange of fluid between neighboring horizontal slices of the drop, so that each slice may be treated as a Lagrangian variable [7]. This description is equivalent to earlier one-dimensional Eulerian lubrication theories [4]. Explicitly, the volume between the bottom of the drop $z(0,t) = z_b(t)$ and z is

$$\xi(z,t) = \int_z^{z_b(t)} \pi r(\zeta,t)^2 d\zeta \qquad (2)$$

In terms of the Lagrangian variable $\xi(z,t)$, we can write the various energy terms for the system as

$$\begin{cases} E_{kin} &= \frac{\rho}{2} \int_0^{\xi_0(t)} \left(\frac{\partial z(\xi,t)}{\partial t} \right)^2 d\xi \\ U_g &= -\rho g \int_0^{\xi_0(t)} z(\xi,t) d\xi \\ U_\Gamma &= \Gamma \int_0^{\xi_0(t)} \sqrt{4\pi z' + \frac{(z'')^2}{(z')^4}} d\xi \end{cases} \qquad (3)$$
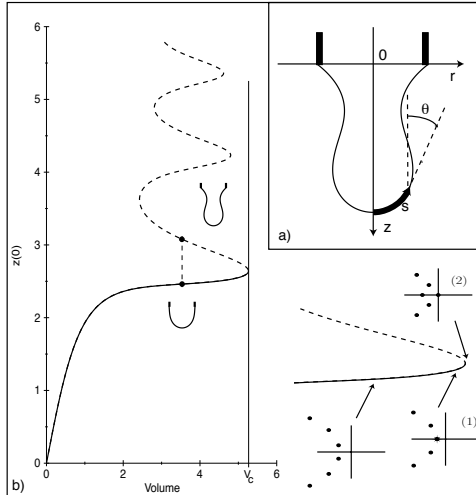

FIG. 1. **a)** Definition of the variables characterizing the drop. **b)** The dimensionless length $z(0)$ versus the dimensionless volume V of the drop. The dashed line corresponds to unstable stationary drops, the solid line to the stable drops. $V_c \approx 5.20$ is the maximum volume of a stationary pendant drop. On the right we show the corresponding eigenvalue spectrum for some representative points close to V_c; the onset of the saddle-node bifurcation is shown in (2), and the leading eigenvalues are $\lambda_1 = 0, \lambda_2 = -0.017 \pm i.3.468$.
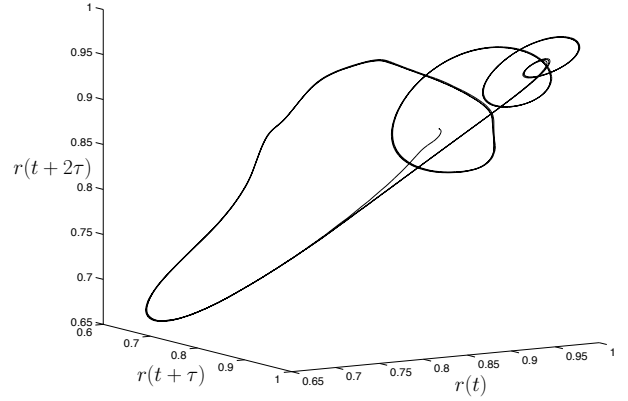

FIG. 2. Reconstruction of the flow by the time delay method, obtained by solving (5) numerically. The radius of the drop is probed at the location $z = 0.5$ and is always continuous. The parameters used for the simulation correspond to a fluid 10 times more viscous than water flowing out of a faucet of diameter $R = 1$ at a flow rate $\epsilon = 0.01$ (in dimensional terms, $R = 2.6mm, \epsilon = 0.015 cm^3/s$). We observe a long excursion followed by a damped oscillations before the orbit returns to the neighborhood of the saddle point.

Here E_{kin} is the kinetic energy, U_g the potential energy, and U_Γ the surface tension energy, $\xi_0(t)$ is the total volume of the drop at the time t, and $(.)' = \partial/\partial\xi$. Then we can write the Lagrangian of the system as $\mathcal{L} = E_{kin} - U_g - U_\Gamma$. The effect of viscosity is expressed in terms of the Rayleigh dissipation function

$$2\mathcal{R} = \dot{E}_{kin} = -3\eta \int_0^{\xi_0(t)} \left(\frac{v'(\xi,t)}{z'(\xi,t)} \right)^2 d\xi \qquad (4)$$

Here η is the dimensionless viscosity in units of $\eta_0 = (\rho\Gamma^3/g)^{1/4}$ ($\eta_0 = 1.627 g/cm.s, \eta = 0.002$ for water), $v = \partial z/\partial t$, and $\dot{E}_{kin}$ is dissipation rate in purely extensional flow. Then, Lagrange's equation for the system is given by $\frac{d}{dt}\frac{\partial\mathcal{L}}{\partial v} = \frac{\partial\mathcal{L}}{\partial z} + \frac{\partial\mathcal{R}}{\partial v}$. For computational facility, we discretize the Lagrangian spatially, characterizing each slice of fluid by the position of its center of mass z_i, velocity $v_i = \frac{\partial z_i}{\partial t}$ and mass m_i, so that for a drop sliced into N disks, we get an N dimensional dynamical system [12], governed by the equations

$$\frac{d}{dt}\frac{\partial\mathcal{L}}{\partial v_i} = \frac{\partial\mathcal{L}}{\partial z_i} + \frac{\partial\mathcal{R}}{\partial v_i}, \quad i = 1, N \qquad (5)$$

We linearize (5) in the neighborhood of the stationary solutions of (1) and evaluate the spectrum $\omega_i, i = 1, N$ of the resulting system. When $V < V_c$, $\mathcal{R}e[\omega_i] < 0$, so that these drops are stable; as $V \approx V_c$ two complex conjugate eigenvalues become real and then one of them reaches the imaginary axis when $V = V_c$. Thus the stationary drop loses its stability

2

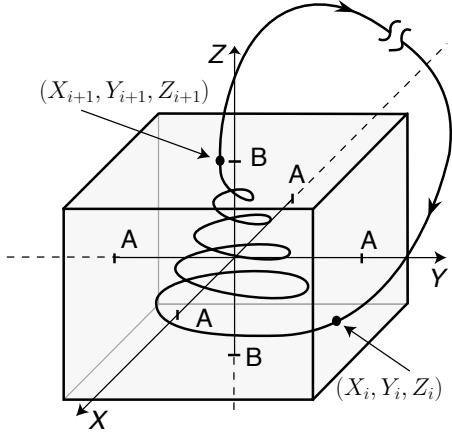by a saddle-node bifurcation, as can be seen in FIG. 1.

FIG. 3. A parallelopiped around the saddle point in phase-space is used to construct the mapping from the plane before the bifurcation to the plane after the bifurcation. A simple rigid rotation is used to model the global reinjection process associated with the complex dynamics of pinch-off, recoil and growth.

In terms of the velocity v_0 of the fluid inside the faucet of radius R, the time scale for the formation of a pendant drop is $\tau_f \sim \frac{R}{v_0}$. Once the volume of the pendant drop is V_c, it forms a neck which quickly narrows down until a droplet pinches off in finite time. This process occurs in a time $\tau_n \sim \sqrt{\rho R^3 / \Gamma}$ [4], independent of the flow rate, and much more rapidly than the time for a drop to form. After a droplet pinches off, the remaining liquid recoils due to capillary forces, oscillating with a characteristic frequency $f = \sqrt{8\Gamma/3\pi\rho\mathcal{V}}$ [13], where $\mathcal{V}$ is the volume of the remaining droplet. Since the volume of the pendant drop grows steadily due to the constant flow rate, this frequency gradually decreases even as the oscilllations are damped out by viscous fluid motions at a rate $1/\tau_d \sim \sqrt{2\pi f \eta}/\mathcal{V}^{1/3}$. For small flow rates, these oscillations are completely damped out by the time the pendant drop attains the critical volume V_c, so that in this case, droplets are emitted from the faucet with a constant periodicity. As the flow rate is increased, these partially damped oscillations modify the onset of the instability via the saddle-node bifurcation. Equivalently, the dimensionless ratio of the filling time to the damping time τ_n/τ_d advances or delays the onset of necking and is responsible for the variation of the periodicity (or lack thereof) of drop emission. For example, as the flow rate is gradually increased, the constant periodicity "drop-drop" gives way to a "drop-drip" scenario via a period-doubling bifurcation as follows. Once the pendant drop reaches the critical volume V_c, a large droplet "drops" leading to

a highly elongated residual filament. If the flow rate is large enough so that the oscillations are not completely damped out, the next droplet will become unstable when $V < V_c$, so that it "drips", leading to a smaller residual filament whose oscillations will be damped out much sooner, thereby (possibly) allowing the pendant drop reach its maximum size V_c before it "drops", and so on.

To build a low-dimensional dynamical system evoking the essence of (5), we solve it numerically over a time much longer than the time for the pinch off of a single droplet, while interrogating it judiciously. Since we need an order parameter that is continuous through the pinch off process, we cannot use the volume and the length of the drop which do not satisfy this criterion. However the radius of the drop at an appropriate location suffices and allows us to rebuild phase space by the delay method [14]. In FIG.2, we show such a reconstruction, and observe that there are two qualitatively different regions: a large excursion corresponding to the dynamics that leads to the pinch-off of a droplet, and a much more compact region corresponding to the damped oscillations following a pinch-off event, that eventually leads the orbit to the neighborhood of the saddle-node bifurcation whence it escapes again. Based on this, we construct a simple model which describes an oscillatory damped mode and a saddle-node bifurcation in the spirit of the Andronov [15]

$$\begin{cases} \partial_t U = (i\omega - \lambda)U \\ \partial_t Z = \epsilon + Z^2 \end{cases} \qquad (6)$$

where $U = X + iY$ is the amplitude of the damped oscillatory mode with eigenvalue $i\omega - \lambda$, with $\lambda > 0$, and $\epsilon > 0$ is the saddle-node bifurcation parameter. In the context of a hydrodynamical theory, U, Z constitute a Galerkin approximation of the complete dynamics, ω and λ are the scaled frequency and the damping rate (in units of $1/t_0$) of the oscillating pendant drop, while ϵ is the scaled flow rate (in units of l_0^3/t_0). Explicitly, this dynamical system can be written in terms of a return map [16] around a parallelopiped of length (A, A, B), centered at the saddle point, as shown in FIG. 3. Then the mapping from the plane $Y = A$ to the plane $Z = B$, maps a point (X_i, A, Z_i) into (X_{i+1}, Y_{i+1}, B) such that

$$X_{i+1} = (X_i \cos(\omega\tau_i) - A\sin(\omega\tau_i))e^{-\lambda\tau_i} \qquad (7)$$
$$Y_{i+1} = (X_i \cos(\omega\tau_i) + A\sin(\omega\tau_i))e^{-\lambda\tau_i} \qquad (8)$$

where

$$\tau_i = \frac{\arctan(B/\sqrt{\epsilon}) - \arctan(Z_i/\sqrt{\epsilon})}{\sqrt{\epsilon}} \qquad (9)$$

In order to complete the formulation of the dynamical model, we need a global reinjection process that

mimics the complex dynamics of pinch-off and recoil of a droplet as it grows. In light of FIG (2), the details of this process are unimportant. The simplest way to model the reinjection flow is via a rigid rotation, as for example,

$$X_{i+1} \rightarrow X_{i+1} \tag{10}$$
$$Y_{i+1} \rightarrow Z_{i+1} \tag{11}$$

The Poincaré map which models the bifurcation is then given by

$$
\begin{cases}
\tau_i &= \dfrac{\arctan(B/\sqrt{\epsilon}) - \arctan(Z_i/\sqrt{\epsilon})}{\sqrt{\epsilon}} \\
X_{i+1} &= (X_i \cos(\omega\tau_i) - A\sin(\omega\tau_i))e^{-\lambda\tau_i} \\
Z_{i+1} &= (X_i \cos(\omega\tau_i) + A\sin(\omega\tau_i))e^{-\lambda\tau_i}
\end{cases} \tag{12}
$$

Numerical simulations of (12), shown in FIG. 4 reveal that for small flow rates all the orbits converge towards a fixed point which describes a periodic dripping process. The same phenomenon appears for large flow rate but it represents a transition from dripping to jetting [17]. For intermediate flow rate, chaotic behavior is observed. In this latter regime, a typical attractor associated with the return map is shown in FIG. 5, agreeing qualitatively with the results of experiments [11].
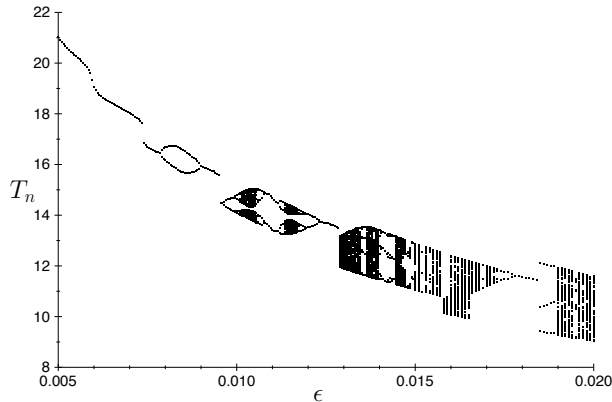

FIG. 4. A phase diagram corresponding to the changes in the dripping behavior as a function of the flow rate ϵ, computed using the return map (12). Very similar diagrams are obtained by solving (5) numerically [7]. For small and large flow rates, the dripping is periodic. For intermediate flow rate, the dripping may be chaotic. The transition to chaos occurs by either a period doubling bifurcation, e.g. $\epsilon = 0.01$, or the result of boundary crisis, e.g. $\epsilon = 0.0125$. For this simulation, the scaled damping rate $\lambda = .17$, and the scaled frequency $\omega = 3.46$.

The structure of the map is self explanatory. As ϵ increases, the observed chaos is connected with the formation of a Smale horseshoe with two symbols. Depending on the value of other parameters such as Z_i and X_i, for larger ϵ the attractor takes the appearence of a spiral, corresponding to a horseshoe with more symbols. The transition to chaos occurs either by succesive period doubling bifurcations or by the collision between a chaotic attractor and an unstable fixed point via a *a boundary crisis* and is responsible for the sudden changes in the attractor [18], similar to that observed in experiments [19,11].

We conclude with a brief discussion of our results. Based on the study of the stability of pendant drop and numerical simulations of a lubrication-type model for the hydrodynamics of a dripping faucet, we constructed a simple return map characterizing the Andronov-Shilnikov bifurcation that accounts for the various experimentally observed behaviors of a dripping faucet, such as the different transitions, the shape of the attractor etc. Possible improvements in the model include a systematic low-dimensional Galerkin projection of the drop dynamics to better estimate the frequency ω and damping rate λ of the oscillatory mode, and a more realistic model for the reinjection process. In a more general context, this model sets up the framework for a study of the problem of chaotic nucleation in different dynamical systems.
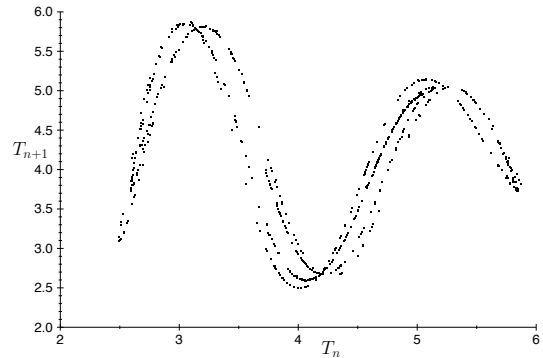

FIG. 5. A return map corresponding to the discrete dynamical system (12), showing the time interval between two consecutive drops T_{n+1} versus the previous such interval T_n, for the same parameters as in FIG. 5. This attractor is characteristic of chaos in the dripping faucet experiment [18,19].

[1] E. Mariotte, *Traité du mouvement des eaux et des autres corps fluides*, E. Michallet, Paris (1686).
[2] T. Young, , *Phil. Trans. R. Soc.*, **95**, 65 (1805).

[3] P.S. Laplace, *Méchanique céleste, suppl. au livre X*, 479 (1805).

[4] J. Eggers, Nonlinear dynamics and breakup of free-surface flows, *Rev. Mod. Phys.*, **69** (3), 865 (1997).

[5] R.S. Shaw, *The dripping faucet as a model chaotic system*, Aerial Press (1984).

[6] A. D'Innocenzo and L. Renna, Modeling leaky faucet dynamics, *Phys. Rev. E,***55**, 6676 (1997).

[7] N. Fuchikami, S. Ishioka and K. Kiyono, Simulation of a dripping faucet, *Phys. Soc. Japan* , **68** (4), 1185 (1999).

[8] J.F. Padday and A.R. Pitt, The stability of axisymmetric menisci, *Phil. Trans. R. Soc. (A),***275**, 489 (1973).

[9] E. Pitts, The stability of a drop hanging from a tube, *J. Inst. Maths. Appl.* **17**, 387 (1976).

[10] D.H. Michael and P.G. Williams, The equilibrium and stability of axisymetric pendent drops, *Proc. R. Soc. Lond. (A)* , **351**, 117 (1976).

[11] T. Katsuyama, K. Nagata, Behavior of the dripping faucet over a wide range of the flow rate, *J. Phys. Soc. Japan* , **68** (2),(1999).

[12] The discretized version of each term in the Lagrangian reads $E_{kin} \simeq \frac{1}{2} \sum_{i=1}^{N} m_i v_i^2$, $U_g \simeq -g \sum_{i=1}^{N} m_i z_i$ $U_\Gamma \simeq \Gamma \sum_{i=1}^{N} \frac{\pi}{2} (r_i + r_{i+1}) \sqrt{(z_{i+1} - z_{i-1})^2 + (r_i - r_{i+1})^2}$, $\dot{E}_{kin} \simeq -3\eta \sum_{i=1}^{N} \left(\frac{v_i - v_{i-1}}{z_i - z_{i-1}} \right)^2 m_i$ where $r_i = \sqrt{\frac{m_i}{\pi(z_i - z_{i-1})}}$ is the average radius of the disk number i, and leads to N equations of motion for each of the disks.

[13] M.S. Longuet-Higgins, B.R. Kerman and K. Lunde, The release of air bubbles from an underwater nozzle, *J. Fluid Mech.*, **230**, 365 (1991).

[14] J.P. Eckmann, D. Ruelle, Ergodic theory of chaos, *Rev. Mod. Phys.* , **57** (3), 617 (1985).

[15] A. Andronov and M. Leontovich, Some cases of dependence of limit cycles on a parameter, *J. State Univ. Gorki*, **6**, 3-24 (in Russian) (1937).

[16] A. Arneodo, P. Coullet, E.A. Spiegel and C. Tresser, Asymptotic chaos, *Physica D* , **14**, 327 (1985).

[17] C. Clanet and J.C Lasheras, Transition from dripping to jetting, *J. Fluid Mech.*, **383**, 307 (1999).

[18] J.C Sartorelli, W.M. Gonçalves and R.D. Pinto, Crisis and intermittence in a leaky-faucet experiment, *Phys. Rev. E* , **49** (5), 49 (1994).

[19] K. Dreyer and F.R. Hickey, The route to chaos in a dripping water faucet, *Am. J. Phys.*, **59** (7), 619 (1991).